Denatured States of Ribonuclease A Have Compact Dimensions and Residual Secondary Structure†

T. R. Sosnick and J. Trewhella*

Life Sciences Division, Los Alamos National Laboratory, Los Alamos, New Mexico 87545

Received March 26, 1992; Revised Manuscript Received June 11, 1992

ABSTRACT: Using small-angle X-ray scattering and Fourier transform infrared spectroscopy, we have determined that the thermally denatured state of native ribonuclease A is on average a compact structure having residual secondary structure. Under strongly reducing conditions, the protein further unfolds into a looser structure with larger dimensions but still retains a comparable amount of secondary structure. The dimensions of the thermally and chemically denatured states of the reduced protein are different but both are more compact than is predicted for a random coil of the same length. These results demonstrate that thermal denaturation in ribonuclease A is not a simple two-state transition from a native to a completely disordered random coil state.

To solve the fundamental problem of determining three-dimensional protein structure from amino acid sequence, the folding pathway must be understood. This is well illustrated by the fact that many possible final states having similar thermodynamic stability can be determined from a given amino acid sequence, though generally only one is the actual end product. The precise nature of the protein folding process remains unclear in part because folding occurs very rapidly and examining partially folded states is extremely difficult. The folding pathway in many proteins has been demonstrated to have intermediates which can be observed using rapid measurement techniques such as kinetic circular dichroism (CD)[1] (Dolgikh et al., 1984; Gilmanshin & Ptitsyn, 1987; Kuwajima et al., 1987) and pulsed proton exchange nuclear magnetic resonance (NMR) (Udgaonkar & Baldwin, 1988) or by chemically trapping various disulfide-linked intermediates (Creighton & Goldenberg, 1984; Weissman & Kim, 1991).

A fundamental issue in the folding process is the relationship between the formation of secondary structure and compaction of the polypeptide. It has been shown that secondary structure elements nucleate before fixed tertiary contacts are formed (Semisotnov et al., 1987; Kuwajima et al., 1987). Chan and Dill (1990) suggested that compaction due to hydrophobic forces, potentially into the putative molten globule state, results in secondary structure formation. But, experimental details concerning the degree of compaction during these initial stages of secondary structure formation and during the final folding into a fixed tertiary structure remain elusive. In order to examine the relationship between secondary structure formation and compaction without the inherent difficulty of measuring the time-dependent folding process, we adopted a strategy that examines the effects of thermal and chemical denaturation along with the importance of disulfide bridges on various states of unfolding of the well-studied, 14-kDa $\alpha + \beta$ protein ribonuclease A (RNase A). To characterize these states, we have examined overall dimensions of the protein using small-angle X-ray scattering (SAXS) and secondary structure content using Fourier transform infrared (FTIR) spectroscopy.

MATERIALS AND METHODS

Sample Preparation. Bovine RNase A was obtained from Calbiochem and further purified using a cation-exchange FPLC column. For all measurements, stock protein solutions, 10–20 mg/mL, were prepared in D_2O with 88 mM MES buffer, pD = 5.7 (uncorrected meter reading). Reducing conditions were obtained by addition of concentrated (1 M) DTT to a final concentration of 100 mM 1 h prior to data collection. Chemical denaturation under reducing conditions was achieved by the addition of GuHCl crystals and concentrated DTT to final concentrations of 6 M GuHCl and 100 mM DTT. D_2O was the solvent of choice in order to optimize conditions for FTIR measurements where it is important to minimize the O–H absorbance peaks that lie in the spectral region of interest. Samples were exchanged into D_2O by repeated lyophilization.

Small-Angle X-ray Scattering. The X-ray scattering data were collected on the small-angle scattering station described in Heidorn and Trewhella (1988). This station uses a line focus from a sealed-tube X-ray source powered by a generator operated at 1.2 kW. The X-rays are focused, using a quartz mirror, onto a lead beam stop mounted directly in front of a one-dimensional position-sensitive detector located 64 cm from the sample. The data were reduced and analyzed as described in Heidorn and Trewhella (1988) and are presented as the scattering intensity per unit solid angle, $I(Q)$, where the momentum transfer, or scattering vector Q, is calculated as

$$Q = \frac{4\pi \sin \theta}{\lambda} \quad (1)$$

λ is the X-ray wavelength, and 2θ is the scattering angle. Guinier analysis (Guinier, 1939) of the very low Q data was used to estimate R_g values and to check for linearity in this regime which is expected for monodisperse samples. More precise structural parameters were derived from a pair-distance distribution function, $P(r)$, analysis which uses scattering data

† This work was performed under the auspices of the DOE (Contract W-7405-ENG-36) and is supported by DOE/Office of Health and Environmental Research Project KP-04-01-00-0.

* Address correspondence to this author.

[1] Abbreviations: BPTI, bovine pancreatic trypsin inhibitor; CD, circular dichroism; d_{max}, maximum linear distance; DTT, dithiothreitol; FTIR, Fourier transform infrared spectroscopy; GuHCl, guanidine hydrochloride; $I(Q)$, scattering intensity per solid angle; MES, 4-morpholineethanesulfonic acid; $P(r)$, pair-distance distribution function; OR, optical rotation; Q, momentum transfer; R_g, radius of gyration; RNase A, ribonuclease A; SAXS, small-angle X-ray scattering; V, volume of the scattering particle; λ, X-ray wavelength; 2θ, scattering angle.

0006-2960/92/0431-8329$03.00/0

over a wider Q range. $P(r)$ functions were calculated according to

$$P(r) = \frac{1}{2\pi^2} \int I(Q) Qr \sin (Qr)\, dQ \qquad (2)$$

using the indirect Fourier inversion algorithm with slit-smearing as described by Moore (1980). The radius of gyration of the scattering particle, R_g, was calculated from the second moment of $P(r)$:

$$R_g^2 = \int r^2 P(r)\, dr / 2 \int P(r)\, dr \qquad (3)$$

Measurement times were between 20 and 30 min with a 15–30-min delay between measurements to ensure temperature equilibration. Temperature was controlled using a water bath and measured using a T-type thermocouple soldered into a brass sample holder.

Fourier Transform Infrared Spectroscopy. FTIR spectra were measured using a Mattson Alpha Centauri spectrometer with 4-cm^{-1} resolution. To minimize the signal-to-noise ratio, 512 scans were coadded and triangularly apodized. The samples were in a Specac Ltd. solution cell with CaF_2 windows and a 0.05-mm Teflon spacer. To minimize interference by the rotational fine structure bands from trace amounts of water vapor, the optical bench was maintained under constant positive dry N_2 pressure. Absorbance spectra were measured after a 30-min purge and ratioed against a single-beam background spectrum collected with no cell. The spectrum of a buffer blank was subtracted from each sample spectrum to give spectra free of contributions from the buffer and cell. Temperature was controlled using a water bath and measured using a T-type thermocouple inserted into a hole drilled into the window of the water-jacketed sample cell.

RESULTS

Small-Angle X-ray Scattering. SAXS data (Figure 1) were used to determine the overall dimensions of RNase A in solution in various states of denaturation. R_g values were calculated from the second moment of $P(r)$ and agreed with those determined from the Guinier analysis (see Materials and Methods and Figure 1, bottom). RNase A under nonreducing conditions maintains a compact shape between room temperature and 61 °C, with an R_g of 15.0 ± 0.2 Å (Figure 2, Table I), identical to that determined for the crystal structure (Wlodawer et al., 1986). By 63 °C, the protein begins to unfold and the transition is complete by 67 °C, at which point R_g has increased by 30% to 19.3 ± 0.9 Å. This R_g value is maintained through the highest temperature measured, which is 81 °C. While the transition is reversible when the sample is heated to 69 °C, we have observed that heating to higher temperatures can result in the refolded dimensions being slightly larger than the initial ones. This observation might be attributed to a small amount of irreversible protein aggregation or to a structural change. This phenomena has previously been observed in Raman spectroscopy experiments (Chen & Lord, 1976).

Additional information on the nature of the unfolding of RNase A is seen in the plots of the pair-distribution functions, $P(r)$ (Figure 3). For a particle of uniform electron density, $P(r)$ is the frequency of vector lengths r connecting small-volume elements within the entire volume of the scattering particle. $P(r)$ goes to zero at the maximum dimension, d_{max}, of the scattering particle. For RNase A under nonreducing conditions the $P(r)$ curves show how the globular protein swells at the transition and d_{max}, increases from 40–45 Å to a final value of 60–65 Å above the transition (Figure 3, upper plot).

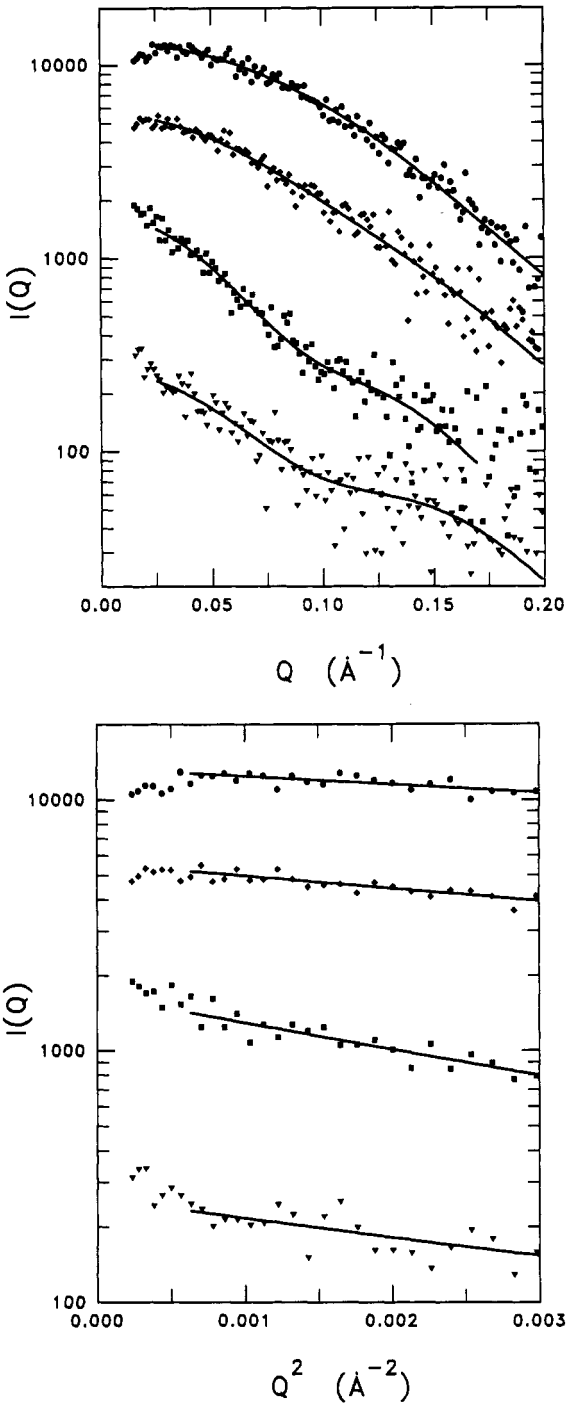

FIGURE 1: Small-angle scattering data for RNase A at 56 °C (circles) and at 67 °C (diamonds) under nonreducing conditions and for RNase A at 57 °C (squares) under reducing conditions. Triangles are data for chemically denatured RNase A under reducing conditions at 22 °C combined with data at 36 °C. (Top panel) Data plotted over the extended Q range. The lines indicate the best-fit $I(Q)$ models used to calculate the $P(r)$ functions shown in Figure 3. The data are offset for clarity. (Bottom panel) Guinier plots for the scattering data. The slope of each line is proportional to $-(R_g^2Q^2/3)$ in the region $QR_g \lesssim 1$. Guinier R_g values were 14.7 ± 0.5, 17.8 ± 0.7, 28.9 ± 2.8, and 22.1 ± 1.9 Å, respectively.

The probability of finding vectors of length ≈ 20 Å within the structure has been reduced with a commensurate increase in probability for distances larger that 45 Å. Above the transition temperature, the protein has lost some tertiary contacts but maintains a shape much more compact than RNase A in a random coil conformation which is expected to have an R_g greater that 41 Å (Miller & Goebel, 1968). The $P(r)$ curve

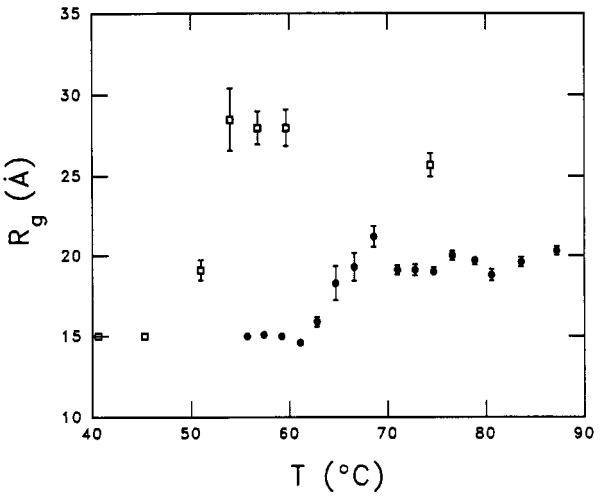

FIGURE 2: Temperature dependence of the radius of gyration, R_g, of RNase A determined using small-angle X-ray scattering under nonreducing (circles) and reducing (squares) conditions.

Table I: Structural Parameters Derived from SAXS[a]

temp (°C)	sample conditions	R_g (Å)	d_{max} (Å)	relative $I(0)$[b]
56	nonreducing	15.0 ± 0.2	40–45	1.0
67	nonreducing	19.3 ± 0.9	60–65	1.11 ± 0.04
45	reducing	15.0 ± 0.2	40–45	1.0
51	reducing	19.1 ± 0.6	60–65	1.02 ± 0.04
56	reducing	28.0 ± 1.0	80–85	1.20 ± 0.07
22 + 36	reducing in 6 M GuHCl	24.1 ± 1.0	65–70	
non specified	reducing in 6 M GuHCl	41[c]	>200	
	random coil model	>43[d]	>200	

[a] From $P(r)$ analysis over the Q range 0.025–Q_{max}, where $R_gQ_{max} \approx$ 4–5. [b] Calculated relative to $I(0)$ for protein below transition under same solvent conditions. The lower contrast of the protein in GuHCl precludes simple comparison of the $I(0)$ measured for this state to that for the native. [c] Data from Tanford et al. (1966). [d] Data from Miller and Goebel (1968).

for a Gaussian random coil with these dimensions has a significant amount of intensity for distances greater than 75 Å (Figure 3, lower plot).

The existence and maintenance of a compact shape by the protein above the transition temperature might be attributed to the presence of the four disulfide bonds between the eight cysteine residues observed in the crystal structure (Wlodawer et al., 1986). These intrachain bonds are arranged topologically such that they alone can constrain the size of the denatured protein. In order to investigate the importance of these disulfide bonds, the scattering measurements were repeated in the presence of a strong reducing agent, 100 mM DTT. At 45 °C, the protein has the same dimensions as the native protein (Figure 2, Table I). At 51 °C, 10 °C less than the previously observed transition, the protein begins to unfold and has shape and dimensions very similar to the structure observed under nonreducing conditions at 67 °C (Figure 3, middle). However, an increase in temperature causes further unfolding into an even more expanded state for temperatures between 54 and 74 °C. In this state, the protein has an R_g of 28 ± 1 Å and d_{max} of 80–85 Å, and the shape of $P(r)$ indicates a significantly extended structure. This structure is, however, still more compact than a Gaussian random coil structure. Unlike the case for the nonreduced protein, thermal denaturation of the reduced protein is an irreversible process and after some time the unfolded protein does aggregate. Potentially, the additional unfolding has exposed more

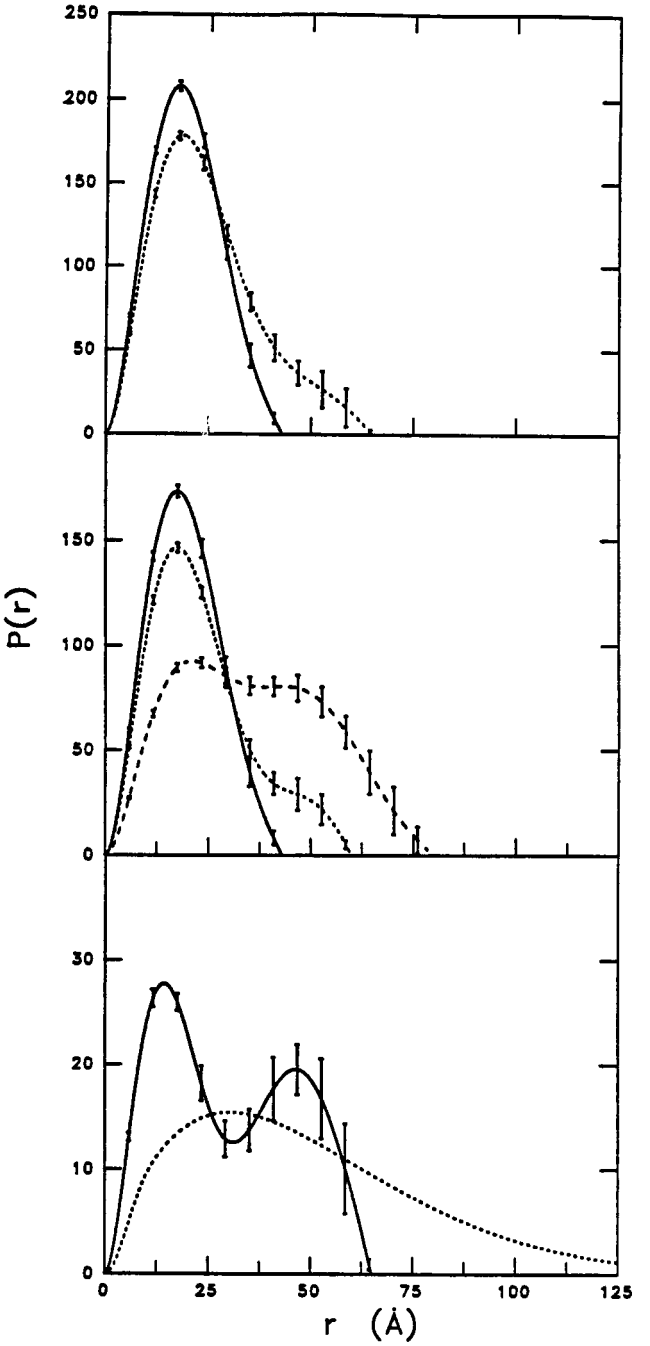

FIGURE 3: (Top) Vector pair-distribution functions, $P(r)$, for RNase A under nonreducing conditions at 57 °C (solid) and 67 °C (dots). (Middle) $P(r)$ functions for RNase A, under reducing conditions, at 45 °C (solid), 51 °C (dots), and 57 °C (dashes). (Bottom) $P(r)$ functions for chemically denatured and reduced RNase A (solid) and for a Gaussian random coil (dots) having an R_g of 41 Å (see text).

hydrophobic residues which lead to additional protein–protein contacts resulting in irreversible aggregation.

The SAXS experiment was repeated again with the protein in 6 M GuHCl and 100 mM DTT to assess the effects of a chemical denaturant under reducing conditions. The high GuHCl content of the solvent increased the mean solvent electron density and greatly reduced the contrast of the protein with respect to the solvent for X-rays; hence measurement times had to be increased to 12 h. Measurements were made at 22 and at 36 °C and the data were identical within the statistical error. The scattering data at the two temperatures were therefore combined (Figure 1) and the resulting R_g and d_{max} for the chemically denatured and reduced RNase A were

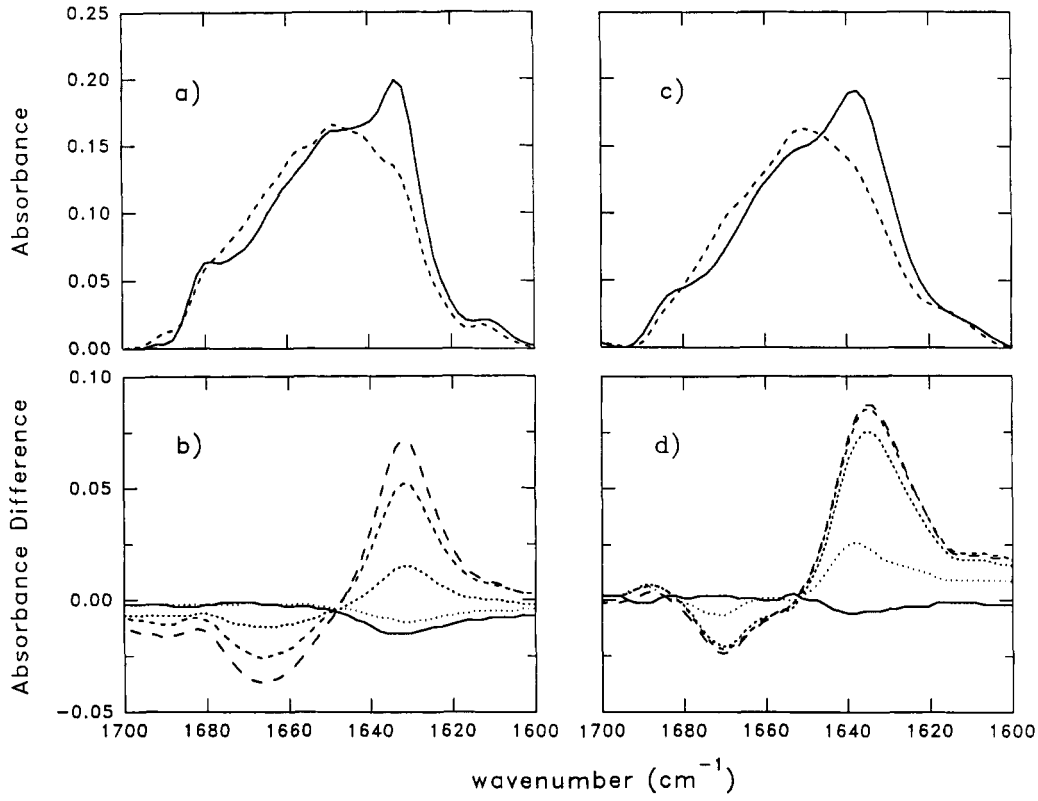

FIGURE 4: Absorbance FTIR spectra for RNase A in the amide I′ region containing bands arising from the carbonyl stretching vibrations contributed by each type of peptide linkage: β-structures (1628, 1637, and 1676 cm^{-1}), turns and bends (1665, 1684, and 1688 cm^{-1}), random coil (1646 cm^{-1}), and α-helix (1655 cm^{-1}). (a) Deconvolved spectra under nonreducing conditions at 54 °C (solid) and 66 °C (dashes). (b) Difference between the raw spectra at 60 °C and at 54 °C (solid), 58 °C (dots), 63 °C (short dashes), 66 °C (medium dashes), and 68 °C (long dashes). (c) Deconvolved spectra for RNase A under reducing conditions at 45 °C (solid) and 54 °C (dashes). (d) Same as (b) but with RNase A under reducing conditions for the difference between the raw spectra at 45 °C and at 42 °C (solid), 51 °C (dots), 54 °C (short dashes), 57 °C (medium dashes), and 60 °C (long dashes).

24.1 ± 1.0 Å and 65–70 Å, respectively (Table I; Figure 3, lower plot). The dimensions of the chemically denatured state were smaller than the thermally denatured protein under reducing conditions (Table I).

Extracting a single shape for the denatured states from the observed $P(r)$ functions is not possible since the functions reflect a time-averaged distribution of what is very likely an ensemble of highly fluctuating structures. The $P(r)$ function for RNase A in 6 M GuHCl is bimodal; however, the signal strength in GuHCl is low, resulting in large error bars in $P(r)$ at distances greater than 25 Å. As a result, the bimodal shape cannot be interpreted in any detail and may very well reflect truncation errors resulting from the poorly determined weak scattering at high Q in this low-contrast sample.

An important concern in interpreting the SAXS data is that the unfolding of the protein might lead to aggregation, perhaps due to the exposure of hydrophobic residues that would normally be buried in the native structure. For aggregated samples the scattering would not be characteristic of individual protein molecules. Aggregated samples characteristically show an upturn in scattered intensity at low Q values in the Guinier regime (i.e., $QR_g \lesssim 1.0$). None of the scattering data show any evidence for such an upturn in the Guinier plots (Figure 1 bottom). For objects having the same mean electron density dissolved in similar solvents, the zero angle scattering intensity, $I(0)$, is proportional to the mass of the scattering particle and hence is very sensitive to the aggregation state of the protein. Since $I(0)$ is determined at each temperature (Table I), one can directly monitor the mass of the scattering particle (Kringbaum & Kugler, 1970) and readily determine if aggregation has occurred. For both reduced and nonreduced RNase, $I(0)$ does increase slightly above the transition (Table I). In the case of the reversible transition for the nonreduced protein, $I(0)$ decreases again to its original value upon cooling. The small increases in $I(0)$ observed upon thermal unfolding precludes any large-scale aggregation and is likely related to solvent layer effects caused by the increase in surface area and the exposure of new residues to solvent ions. Consistent with this interpretation is the fact that a decrease in probability is observed in the $P(r)$ functions at small r values for the unfolded states. Protein aggregation would produce the opposite effect.

FTIR Spectroscopy. FTIR spectroscopy was used to measure the secondary structure content of the protein in the various states of denaturation characterized in the scattering experiments. Secondary structure content estimates were based upon absorption at 11 well-defined frequencies in the deuterium-shifted amide I (amide I′) region (1620–1700 cm^{-1}) of the FTIR spectrum (Byler & Susi, 1986). This region primarily contains bands attributable to the carbonyl stretching vibrations contributed by each type of peptide linkage.

The resolution enhanced (by Fourier deconvolution) spectra for the native and thermally denatured protein under nonreducing and reducing conditions are shown in Figure 4. A strong peak at about 1633 cm^{-1} is observed in the spectra below the transition temperature in both the presence and absence of reducing agent. This peak is attributable to β-sheet component which, according to the crystal structure, comprises approximately half of the secondary structure content. There is a slight change in the location and width of this peak under reducing conditions which might be due to

the loss of a disulfide bond in a loop region connecting two β strands, which could slightly alter the stretching frequency. Under both nonreducing and reducing conditions, the spectra change quite rapidly over the same temperature ranges for which unfolding was observed in the SAXS experiments. Importantly, in the spectra of the denatured protein for both conditions, there is a broad spread of the amide I′ band which is indicative of the presence of different types of secondary structural elements, and the band at 1633 cm^{-1} specifically indicates residual β-sheet structure.

For many proteins, it is possible to fit the FTIR spectrum with multiple Gaussian peaks and assign percentages of each type of secondary structure based upon the location and area of each peak. However, even deconvolved spectra for RNase A are sufficiently featureless that curve fitting in the region 1640–1680 cm^{-1} could not be done reliably. Consequently, we have chosen the native state as a starting point and have presented the differences between the raw spectra for the protein just below the transition temperature and at the other temperatures (Figure 4). Under both nonreducing and reducing conditions, the difference spectra change minimally below the transition temperatures. Across the previously determined transition temperatures, however, there are a number of significant changes. In particular, the spectra show a loss of approximately a third to a half of the peak area at 1633 cm^{-1}, assignable to β-sheet structure, and a comparable increase in area in the region between 1650 and 1680 cm^{-1}. This latter region can contain peaks assignable to turns and bends, random coil, β-sheet, and α-helix structures. Under both nonreducing and reducing conditions, very similar changes in the spectra are observed upon denaturation. The FTIR spectra show that both the unfolded structures have residual secondary structure that is not assignable to random coil. Due to the high ^1H content of GuHCl, FTIR measurements could not be performed on the protein in GuHCl.

DISCUSSION

The SAXS data indicate smaller average dimensions for the thermally (R_g = 28 ± 1 Å) and the chemically (R_g = 24 ± 1 Å) denatured states of RNase A under reducing conditions than previously reported. Tanford et al. (1966) measured the viscosity of RNase A solution with 6 M GuHCl under reducing conditions where it is believed that the protein is in a completely random coil conformation (Aune et al., 1967) and determined a root-mean-square end-to-end distance, $\langle r^2 \rangle_0$, of 101 Å which equates to an R_g of 41 Å, using the relationship $\sqrt{6}R_g = \langle r^2 \rangle_0$ applicable for random coils (Miller & Goebel, 1968). Furthermore, Miller and Goebel (1968) calculated the dimensions for a random coil model that incorporated the geometrical constraints imposed by the amino acid composition of RNase A and determined values that were slightly greater than those of Tanford. The current work shows that each form of the denatured protein studied maintains an average shape less extended than expected for a Gaussian random coil polypeptide. It should be noted here that SAXS data represent the ensemble- and time-averaged structure for the molecules in a solution, and hence the structural parameters derived may arise from a composite of multiple conformations. For a denatured protein in solution it seems highly likely that there will be multiple conformations present.

Since the FTIR measurements indicate that residual secondary structure remains in the thermally denatured states, it is not surprising that we observe $P(r)$ functions that indicate the structure is more compact than a random coil. The chemically denatured state is more complex as the extent of residual structure is uncertain (Dill & Shortle, 1991). Whether a denatured protein obtains a random coil structure depends upon the nature of the solvent. In the terminology of polymer chemistry, there exist "good", "bad", and "θ" solvents which affect the degree of compaction and structure of denatured states (Dill & Shortle, 1991). We find that RNase A in 6 M GuHCl is more compact than a Gaussian random coil. Similar behavior has been observed for lysozyme in 6 M GuHCl under reducing conditions where it behaves as a 75-Å-diameter sphere as determined by diffusion measurements using optical mixing spectroscopy (Dubin et al., 1973).

The SAXS and FTIR data demonstrate that the final state of thermal denaturation of RNase A is a state which remains compact and has residual secondary structure. Flanagan et al. (1992) observed similar results for a staphylococcal nuclease mutant that was partially unfolded. There is an increase in the partial heat capacity at the melting transition in proteins which Privalov et al. (1989) suggest is due to the exposure of internal nonpolar groups to water rather than the complete loss of secondary structure. This interpretation is consistent with the 30% increase in R_g and the residual secondary structure observed in our measurements for the nonreduced RNase A. This small increase in linear dimensions has also been observed using light scattering spectroscopy (Nicoli & Benedek, 1976). When a strong reducing agent is added, RNase A unfolds further into another more extended state but still has a comparable amount of ordered secondary structure. Thus, at least two distinct states have been identified upon thermal denaturation and the end product is not a random coil. The current data are therefore inconsistent with thermal denaturation as a simple two-state "all-or-none" cooperative transition from a native to a completely unfolded state. Other experiments on RNase A performed under nonreducing conditions have examined the effects of thermal denaturation on enzyme activity (Nall & Baldwin, 1977) and structure (Nicoli & Benedek, 1976). A smooth sigmoidal change was observed in these properties from an initial to a final value which was interpreted according to a two-state unfolding transition without any intermediate states. Likewise, in the current measurements, under nonreducing conditions, changes are observed in the dimensions which could also be interpreted according to a two-state transition; however, we stress, the end state of thermal denaturation is not a completely unfolded random coil structure. The transition that is being measured is one from the native state to a state where biological function has been lost along with some degree of compactness and secondary structure.

The significant amount of β-sheet remaining upon thermal denaturation of RNase A has been both predicted (Burgess & Scheraga, 1975) and observed using Raman spectroscopy (Chen & Lord, 1976). Residual secondary structure upon thermal denaturation has also been observed in many other proteins using optical rotation (OR) (Aune, 1967) or CD spectroscopy (Kuwajima et al., 1985). In apparent contradiction with our FTIR results, Labhardt (1982) concluded that there was no residual β-sheet structure in RNase A upon thermal denaturation on the basis of CD data. However, those data were collected in the range 212–250 nm, and accurate assessment of β structure requires that data be measured to at least 180 nm (Johnson, 1988). Privalov et al. (1989) also performed CD measurements on various states of RNase A: thermally denatured with and without intact disulfide bonds and chemically denatured with 6 M GuHCl. While they interpret their data to indicate little residual

structure in any of these states, they did observe in both thermally denatured states a significant amount of negative helicity in the region 210–240 nm that was not observed in the spectrum of the chemically denatured state. According to Johnson (1988), this negative intensity can only be accounted for by the existence of α-helix or β-sheet. We suggest that these CD spectra for RNase A in the thermally denatured states, with and without reducing agents, are consistent with our results indicating a combination of β-sheet and random coil structures. Robertson and Baldwin (1991) also observed a residual CD signal in thermally denatured RNase A.

NMR methods have also been used to examine the denaturation of RNase A. Rapid mixing ^{1}H-NMR experiments on chemically denatured RNase A (Udgaonkar & Baldwin, 1988) showed that, during folding, stable intermediates with β-sheet structures are formed before any tertiary contacts. In thermal denaturation experiments at temperatures above the melting temperature, Rico et al. (1989) determined that the ^{1}H resonances are essentially those corresponding to a cross-linked random coil. However, they as well as Talluri and Scheraga (1990) noticed a degree of protection from exchange with the D_2O solvent for some amide protons at pH = 2.5, including those in proposed β-sheet folding initiation site in residues 106–118. Using similar methods, Robertson and Baldwin (1991) also observed a degree of protection for a number of residues at pD $\leq$ 3.8, primarily valine and isoleucine. However, they proposed that the intrinsic exchange rates upon which protection is based are too high for these two residues and hence concluded that no stable hydrogen-bonded structure remained upon thermal denaturation. This apparent discrepancy might be reconciled by noting that the current measurements were performed under more neutral conditions (pD = 5.7), and thermal denaturation under acidic conditions has been shown to result in an increased loss of secondary structure in proteins (Privalov et al., 1989).

It should be stressed that, like CD, FTIR measurements are macroscopic in nature and are examining a time-averaged structure. The possibility remains that the residual structure observed using FTIR might be the result of fluctuating structures which would not give rise to a high degree of solvent protection. It is also possible that the residual secondary structure might not be nativelike. With FTIR, like CD spectroscopy, it is not possible to determine the origin of the residual signal, which in the case of FTIR spectroscopy is sensitive to the H-bonding of the carbonyl oxygen. The significant fact remains that the FTIR and the aforementioned OR, CD, and Raman measurements do indicate that residual structure exists in thermally denatured RNase A. The origin of this structure remains an open issue (Robertson & Baldwin, 1991).

The term molten globule has been used to describe denatured states and folding intermediates for a number of proteins (Kuwajima, 1989; Ptitsyn et al., 1990) but the definition of the term varies depending upon context. The theoretical properties of the molten globule state include nativelike secondary structure and a dense interior with linear dimensions only slightly larger, $\approx$10%, than found in the native structure (Ptitsyn, 1987; Finkelstein & Shakhnovich, 1989). To avoid confusion, we will follow the suggestion of Kim and Baldwin (1990) that the term molten globule be reserved for states having these theoretical properties and that the term "collapsed form" be used to describe the more generally observed states whose properties are not as well defined.

The observed nonreduced state of RNase A does have a significant amount of residual secondary structure, but it is quite expanded, having linear dimensions larger than the native structure by a third. This state is too large and, on the basis of calorimetric data, probably has a core too exposed to solvent (Privalov et al., 1989) to be a molten globule as defined above. Furthermore, the thermally denatured state of reduced RNase A has linear dimensions a factor of 2 larger than the native structure and certainly cannot be considered to be in the molten globule state. Both these states are more compact than a random coil structure and fall into the category of collapsed forms. The existence of secondary structure in these two collapsed states indicates that a complete hydrophobic collapse with a dense, solvent-excluded hydrophobic core is not required for secondary structure formation.

The existence of comparable amounts of secondary structure in the thermally denatured and reduced state and in the thermally denatured nonreduced state suggests that complete disulfide bond formation is not required for secondary structure formation. Thus, the nucleation of folding can begin at the local level before all the disulfide bonds have formed. The disulfide bonds might then serve to tether existing regions of ordered secondary structure together. The pathway to native disulfide bond formation is not clearly understood. Creighton (1977) originally proposed that nonnative disulfide bonds are formed on the folding pathway in bovine pancreatic trypsin inhibitor (BPTI). Recently, Weissman and Kim (1991) proposed that only native disulfide linkage intermediates are important in the folding pathway of BPTI and the nonnative linkages are dead-end excursions off the main pathway. However, this proposed pathway has the requirement that, in the late stages of folding, the protein must substantially rearrange in order to make the third and final linkage (Hoffman, 1991). Under reducing conditions, we observe that the thermally denatured state of RNase A is quite expanded, but still a degree of ordered secondary structure remains. Thus, a folding protein might have ordered subunits which are well separated and substantial rearrangement of these subunits may be possible.

ACKNOWLEDGMENT

We thank J. Bryngelson for many useful discussions and for critically reading the manuscript and Robert Woody for discussions on interpretation of the FTIR data.

REFERENCES

Aune, K. C., Salahuddin, A., Zarlengo, M. H., & Tanford, C. (1967) *J. Biol. Chem. 242*, 4486.
Burgess, A. W., & Scheraga, H. A. (1975) *J. Theor. Biol. 53*, 403.
Byler, D. M., & Susi, H. (1986) *Biopolymers 25*, 469.
Chan, H. S., & Dill, K. A. (1990) *Proc. Natl. Acad. Sci. U.S.A. 87*, 6388.
Chen, M. C., & Lord, R. C. (1976) *Biochemistry 15*, 1889.
Creighton, T. E. (1977) *J. Mol. Biol. 113*, 329.
Creighton, T. E., & Goldenberg, D. P. (1984) *J. Mol. Biol. 179*, 497.
Dill, K. A., & Shortle, D. (1991) *Annu. Rev. Biophys. Biophys. Chem. 60*, 795.
Dolgikh, D. A., Kolomiets, A. P., Bolotina, I. A., & Ptitsyn, O. B. (1984) *FEBS Lett. 165*, 88.
Dubin, S. B., Feher, G., & Benedek, G. B. (1973) *Biochemistry 12*, 714.
Finkelstein, A. V., & Shakhnovich, E. I. (1989) *Biopolymers 28*, 1681.
Flanagan, J. M., Kataoka, M., Shortle, D., & Engelman, D. M. (1992) *Proc. Natl. Acad. Sci. U.S.A. 89*, 748.
Gilmanshin, R. I., & Ptitsyn, O. B. (1987) *FEBS Lett. 223*, 327.
Guinier, A. (1939) *Ann. Phys. (Paris) 12*, 161.

Heidorn, D. B., & Trewhella, J. (1988) *Biochemistry 27*, 909.
Hoffman, M. (1991) *Science 253*, 1357.
Johnson, W. C. (1988) *Annu. Rev. Biophys. Biophys. Chem. 17*, 145.
Kim, P. S., & Baldwin, R. L. (1990) *Annu. Rev. Biochem. 59*, 631.
Kringbaum, W. R., & Kugler, F. R. (1970) *Biochemistry 9*, 1216.
Kuwajima, K. (1989) *Proteins: Struct., Funct., Genet. 6*, 87.
Kuwajima, K., Hiraoka, Y., Ikeguchi, M., & Sugai, S. (1985) *Biochemistry 24*, 874.
Kuwajima, K., Yamaya, H., Miwa, W., Sugai, S., & Nagamura, T. (1987) *FEBS Lett. 221*, 115.
Labhardt, A. M. (1982) *J. Mol. Biol. 157*, 331.
Miller, W. G., & Goebel, C. V. (1968) *Biochemistry 7*, 3925.
Moore, P. B. (1980) *J. Appl. Crystallogr. 13*, 168.
Nall, B. T., & Baldwin, R. L. (1977) *Biochemistry 16*, 3572.
Nicoli, D. F., & Benedek, G. B. (1976) *Biopolymers 15*, 2421.
Privalov, P. L., Tiktopulo, E. I., Venyaminov, S. Yu., Griko, Yu. V., Makhatadze, G. I., & Khechinashvili, N. N. (1989) *J. Mol. Biol. 205*, 737.
Ptitsyn, O. B. (1987) *J. Protein Chem. 6*, 273.
Ptitsyn, O. B., Pain, R. H., Semisotnov, G. V., Zerovnik, E., & Razgulyaev, O. I. (1990) *FEBS Lett. 262*, 20.
Rico, M., Bruix, M., Santoro, J., Gonzalez, C., Neira, J. L., Nieto, J. L., & Herranz, J. (1989) *Eur. J. Biochem. 183*, 623.
Robertson, A. D., & Baldwin, R. L. (1991) *Biochemistry 30*, 9907.
Semisotnov, G. V., Rodionova, N. A., Kutyshenko, V. P., Ebert, B., Blanck, J., & Ptitsyn, O. B. (1987) *FEBS Lett. 224*, 9.
Talluri, S., & Scheraga, H. A. (1990) *Biochem. Biophys. Res. Commun. 172*, 800.
Tanford, C., Hawahara, K., & Lapanje, S. (1966) *J. Biol. Chem. 241*, 1921.
Udgaonkar, J. B., & Baldwin, R. L. (1988) *Nature 335*, 694.
Weissman, J. S., & Kim, P. S. (1991) *Science 253*, 1386.
Wlodawer, A., Borkakoti, N., Moss, D. S., & Howlin, B. (1986) *Acta Crystallogr., Sect. B 42*, 379.